Thayer, W. S., & Rubin, E. (1981) *J. Biol. Chem. 256*, 6090–6097.
Waring, A. J., Rottenberg, H., Ohnishi, T., & Rubin, E. (1981) *Proc. Natl. Acad. Sci. U.S.A. 78*, 2582–2586.
Waring, A. J., Rottenberg, H., Ohnishi, T., & Rubin, E. (1982) *Arch. Biochem. Biophys. 216*, 51–61.
Wing, D. R., Harvey, D. J., Belcher, S. J., & Paton, W. D. M. (1984) *Biochem. Pharmacol. 33*, 1625–1632.

Penetration of a Cardiotoxin into Cardiolipin Model Membranes and Its Implications on Lipid Organization†

A. M. Batenburg,*,‡ P. E. Bougis,§ H. Rochat,§ A. J. Verkleij,∥ and B. de Kruijff∥

Laboratory of Biochemistry and Institute of Molecular Biology, State University of Utrecht, Transitorium III, Padualaan 8, De Uithof, Utrecht, The Netherlands, and UA 553 CNRS et V 172 INSERM, Laboratoire de Biochemie, Faculté de Médecine, Secteur Nord, 13326 Marseille Cedex 15, France

Received May 15, 1985

ABSTRACT: The interaction of cardiotoxin II of *Naja mossambica mossambica* with cardiolipin model membranes was investigated by binding, fluorescence, resonance energy transfer, fluorescence quenching, ^{31}P NMR, freeze–fracture, and small-angle X-ray experiments. An initially electrostatic binding appeared to be accompanied by a deep penetration, most likely into the acyl chain region of the phospholipids, indicating a hydrophobic contribution to the strong interaction ($K_D \simeq 5 \times 10^{-8}$ M). This binding results in a fusion of unilamellar vesicles as indicated by a fluorescence-based fusion assay, freeze–fracture, and X-ray diffraction. In these fused structures freeze–fracture electron microscopy reveals the appearance of particles, which is accompanied by the induction of an isotropic component in ^{31}P NMR. The well-defined particles are interpreted as inverted micelles, and the localization of the cardiotoxin molecule in these structures is discussed.

Proteins and phospholipids are the major components of biological membranes and for a proper functioning of the membranes lipid–protein interactions appear to be essential. One aspect of these interactions is the modulation by proteins of local lipid structure. Protein-induced nonbilayer lipid structures (lipidic particles, short inverted H_{II} cylinders) have been suggested to play a role in essential processes as transbilayer transport of lipids, membrane fusion, and translocation of newly synthesized proteins across membranes (Nesmeyanova, 1982; de Kruijff et al., 1981; Cullis & Hope, 1978).

Model membrane experiments revealed that lipid polymorphism can be modulated by the hydrophobic peptide gramicidin and the membrane spanning part of the intrinsic protein glycophorin. Whereas gramicidin displays a strong bilayer destabilizing action, for instance in the typical bilayer system of dioleoylphosphatidylcholine (Van Echteld et al., 1981, 1982), even when added through the aqueous phase (Killian et al., 1984), glycophorin in contrast stabilizes the bilayer structure in H_{II} phase preferring lipid systems of dioleoylphosphatidylethanolamine (Taraschi et al., 1982) and Ca^{2+}–cardiolipin (Taraschi et al., 1983). Extrinsic proteins too are able to affect macroscopic lipid structure. In the beef heart cardiolipin system, poly(L-lysine) with a polymerization degree of $n = 120$ down to $n = 5$ was found to stabilize bilayer structure in the presence of Ca^{2+}, a strong inducer of H_{II} formation in pure cardiolipin (de Kruijff & Cullis, 1980a; B. de Kruijff, unpublished observations). On the other hand, cytochrome *c*, a basic protein with eight net positive charges, was observed to induce inverted structures in cardiolipin-containing systems (de Kruijff & Cullis, 1980b) and must in this respect be marked a bilayer destabilizer.

These results suggest that the effects of proteins and polypeptides on lipid polymorphism cannot directly be correlated to overall positive charge or hydrophobicity but that more subtle features, for instance, the spacial distribution of the charged amino acids and the three-dimensional structure of the protein, are important. For a better understanding of the relative importance of these features it is fundamental to study the interaction of well-defined peptides with lipid model membranes.

Among the natural peptides having a high affinity for certain membrane lipids are the cardiotoxins from snake venoms. The cardiotoxins form a group of highly basic proteins consisting of 60–61 amino acid residues, giving the protein a molecular weight of about 7000 (Dufton & Hider, 1983). Besides positively charged residues, the toxins contain some hydrophobic stretches, especially the sequence 6–11. The tertiary structure, which is believed to contain three loops forming an extended β-sheet (Lauterwein & Wüthrich, 1978), is firmly stabilized by four disulfide bridges. On the basis of the high amount of cardiotoxin that was observed to be bound to biological membranes, it was proposed that lipids were involved in this binding (Vincent et al., 1976), and this opened the way for studies of cardiotoxin–phospholipid interactions (Bougis et al., 1983). It was established that the cardiotoxins bind only to negatively charged phospholipids (Dufourcq & Faucon, 1978; Vincent et al., 1978), indicating a strong electrostatic component in the interaction. On the other hand, the sequence around tryptophan 11 is believed to leave its aqueous environment upon binding, explaining the blue shift and increased intensity of the tryptophan fluorescence (Du-

† The investigations were carried out under the auspices of the Netherlands Foundation for Chemical Research (S.O.N.) and with financial aid from The Netherlands Organization for the Advancement of Pure Research (Z.W.O.).
‡ Laboratory of Biochemistry.
§ UA 533 CNRS et V 172 INSERM.
∥ Institute of Molecular Biology.

0006-2960/85/0424-7101$01.50/0

fourcq & Faucon, 1978; Vincent et al., 1978). Raman spectroscopy and diphenylhexatriene fluorescence polarization experiments indicated a strong influence on lipid chain order (Faucon et al., 1981, 1983), while on the contrary protein structure remained unaffected (Pézolet et al., 1982). The monomolecular film technique was used to obtain data concerning the specificity of cardiotoxin penetration into phospholipid monolayers (Bougis et al., 1981).

Very little effort has been paid until now to a structural analysis of the cardiotoxin–lipid complexes. A first electron microscopy study (Gulik-Krzywicki et al., 1981) revealed that indeed supramolecular lipid structure was severely affected by cardiotoxin. However, this observation was made on a natural total lipid extract of rather complex composition. For a better interpretation of the observed nonbilayer lipid structures that are interesting in light of the above-mentioned modulation of lipid structure by proteins, it is necessary to study better defined model membranes. In the present study, the cardiotoxin II–lipid interaction was studied with beef heart cardiolipin. This lipid was chosen because it shows an interesting isothermal polymorphism (de Kruijff et al., 1985), modulated by divalent cations as well as by certain positively charged proteins as mentioned above.

The nature of the cardiotoxin–cardiolipin interaction was studied with a variety of techniques. The depth of penetration of the toxin into the lipid model membranes was investigated by fluorescence techniques using the intrinsic tryptophan probe and membranous and aqueous quenchers of its fluorescence. Structural analysis of the peptide–lipid complex was performed by ^{31}P NMR, small-angle X-ray diffraction, and freeze–fracture electron microscopy. Cardiotoxin was found to induce fusion of cardiolipin vesicles. This fusion was further characterized by fusion assays based on the mixing of aqueous vesicle contents and of vesicle lipids.

The results of these studies give us a coherent picture of the alterations in lipid structure induced by cardiotoxin. The localization of the toxin molecules in these structures is discussed.

Materials and Methods

Materials. Cardiolipin sodium salt from beef heart, N-Rh-PE,[1] and N-NBD-PE were obtained from Avanti (Birmingham, AL). Egg PC was isolated from hen egg yolks by standard procedures, and egg phosphatidylglycerol was prepared from egg PC (Comfurius & Zwaal, 1977).

Cardiotoxin II (CTX II or V_2^{11}; Louw, 1974) was isolated from the venom of *Naja mossambica mossambica* (Bougis et al., 1983) and purified on antiphospholipase A_2 γ-globulin–Sepharose CL-4B (Delori & Tessier, 1980). The toxin samples thus obtained exhibited no phospholipase activity in the buffers used, even at high protein to lipid ratios during prolonged incubations of 48 h at 25 °C, as judged from the absence in thin-layer chromatography of lyso compounds or free fatty acids. The necessity of such a purity is demonstrated by the serious artifacts caused by phospholipase traces in melittin–phospholipid systems (Dasseux et al., 1984). All other chemicals were at least of analytical grade.

Model Membranes. Multilamellar vesicles (MLV) were obtained by hydrating the dry lipid film as described before (de Kruijff & Cullis, 1980b). Small unilamellar vesicles (SUV) were prepared from MLV by sonication with a Branson B12 sonifier equipped with a 0.5-in. flat-top disruptor tip under nitrogen in ice–water for 10 times 30 s at 50 W and isolated as the supernatant of a 10-min centrifugation at 27000*g*. Large unilamellar vesicles (LUV) were prepared by the reverse-phase evaporation technique (Szoka & Papahadjopoulos, 1978) with the modifications described before (Wilschut et al., 1980). Shortly, vesicles are prepared by sonicating 0.3 mL of buffer with 7.5 mg of lipid in 1 mL of diethyl ether in a bath-type sonicator, followed by a stepwise evaporation of the ether. The vesicles are "sized" by extrusion through a 0.2-μm polycarbonate Unipore membrane. All vesicles were prepared and all experiments were performed in 100 mM NaCl, 10 mM cacodylate hydrochloride, and 1 mM EDTA, pH 7.0, 25 °C, unless otherwise stated.

Binding Studies. The protein–lipid binding experiments were carried out by incubating 200 nmol of cardiolipin–MLV with protein at 30 °C for 30 min in a total volume of 150 μL of buffer. The nonbound protein was separated by centrifugation in a Sorvall RCB-2 at 27000*g* for 20 min at 4 °C and was determined in the supernatant. The amount of lipid in the supernatant was neglectable, and incubations without lipid gave 100% recovery of the protein in the supernatant.

Intrinsic Fluorescence Measurements. For measurements of the changes of intrinsic fluorescence of tryptophan upon lipid binding, different amounts of SUV were added to a 10 μM cardiotoxin II solution. After 3 min, an emission spectrum was recorded with a Perkin-Elmer MPF 3 fluorometer, the excitation wavelength being 280 nm. The percentual increase in fluorescence intensity at a fixed wavelength was calculated after correction for volume change.

Tryptophan to Anthracene Resonance Energy Transfer Measurements. The energy transfer from peptide tryptophan to membrane-incorporated anthracene can be used to study peptide insertion (Uemura et al., 1983). Anthracene was added to the lipid solution in chloroform prior to the preparation of the dry film. The obtained SUV contained anthracene and phospholipid in a molar ratio of 1:80 on the basis of lipid phosphorus. Emission spectra were recorded with a Perkin-Elmer MPF 3 fluorometer 3 min after addition of CTX II, the excitation monochromator being set at 280 nm.

Fluorescence Quenching Experiments. The tryptophan fluorescence at 340 nm of 10 μM CTX II was quenched by titration with aliquots of a 3 M acrylamide or 4 M potassium iodide solution in buffer. In the case of iodide, the titrant also contained 1 mM $Na_2S_2O_3$ to prevent I_3^- formation. If the quenching was studied in the presence of lipids, titration was started 3 min after addition of the SUV.

^{31}P NMR. ^{31}P NMR spectra were recorded at 81.0 MHz with a Bruker WP 200 under conditions of proton decoupling as described before (Cullis & de Kruijff, 1976). Typically, 5000 45° pulses with a 1-s interpulse time were employed on 1-mL samples containing 20 μmol of lipid MLV (based on P_i) to which increasing amounts of CTX II as aliquots of a 15 mM solution in buffer were added. In these experiments the buffer contained 50 mM cacodylate to improve buffer capacity and 25% ^2H_2O. To increase the signal to noise ratio, the free induction decays were exponentially filtered, resulting in a 50-Hz line broadening.

Small-Angle X-ray Diffraction. SUV (5 μmol of lipid) were added to 10 mL of CTX II containing buffer. The samples were spun for 10 min at 27000*g* at 4 °C and the pellets brought into the 1 × 1.5 × 16 mm slits of the sample holders. The holders were closed with cellophane and mounted into a Kratky

[1] Abbreviations: CTX, cardiotoxin; EDTA, ethylenediaminetetraacetic acid; LUV, large unilamellar vesicles; MLV, multilamellar vesicles; N-Rh-PE, *N*-(lissamine rhodamine B sulfonyl)dioleoylphosphatidylethanolamine; N-NBD-PE, *N*-(7-nitro-2,1,3-benzoxadiazol-4-yl)phosphatidylethanolamine; PC, phosphatidylcholine; SUV, small unilamellar vesicles.

small-angle X-ray camera whose position-sensitive LETI detector was interfaced to a microcomputer. The samples were irradiated for ca. 10 min with a 10 × 0.2 mm copper K_α beam (4 kV, 20 mA).

Freeze–Fracture Electron Microscopy. A total of 50 μL of CTX II containing buffer was added to 100 μL of 50 mM cacodylate buffer, containing SUV (2 μmol of lipid). The samples were frozen either in the presence of glycerol as cryoprotectant or without cryoprotectant by the one-sided jet-freezing technique (Pscheid et al., 1981).

Extraction Experiments. A total of 20 nmol of CTX II in 100 μL of buffer was added to 430 μL of chloroform/methanol, 5:8 (v/v), containing about 450 nmol of lipid phosphorus. Phase separation was induced by addition of 370 μL of chloroform and 100 μL of buffer, followed by a 10-min 27000*g* centrifugation.

Fusion Studies. Two types of fusion experiments were performed. One of them, studying the mixing of aqueous vesicle contents (Wilschut et al., 1980), can shortly be described as follows. Tb^{3+}–citrate complex and dipicolinic acid (DPA) were enclosed in different populations of LUV, and the formation of the fluorescent $Tb(DPA)^{3-}$ complex upon addition of a fusogen was followed in time, while EDTA present in the extravesicular medium prevented formation of the complex outside the vesicles. In these experiments, a buffer containing 2 mM L-histidine and 2 mM 2-[[tris(hydroxymethyl)methyl]amino]ethanesulfonic acid, pH 7.4, was used. In the second assay (Struck et al., 1981), the mixing of the lipids of two different vesicle populations was followed, making use of resonance energy transfer. One population containing 3% on basis of lipid phosphorus of both fluorescent lipid analogues N-Rh-PE and N-NBD-PE was mixed with pure cardiolipin vesicles in a ratio of 1:19 (based on P_i). The decreasing fluorophore density during fusion is reflected in a less efficient resonance energy transfer, measured as an increase of N-NBD fluorescence. For reasons of comparison a 100% fusion value was established by measuring the fluorescence of a third vesicle population, containing cardiolipin, N-Rh-PE, and N-NBD-PE in a ratio of 99.7:0.15:0.15, to which a saturating amount of CTX II was added in order to obtain lipid–protein structures of comparable structure. To correct for the increase in light scattering upon addition of CTX II, blanks were always subtracted, obtained by measuring the effect of addition of the protein to nonfluorescent lipid vesicles.

Routine Procedures. Phospholipid was determined as inorganic phosphate after destruction with perchloric acid (Fiske & Subbarov, 1925; Rouser et al., 1975). Protein was determined by a modified Lowry assay (Peterson, 1973).

RESULTS

Binding Studies. Binding of CTX II to cardiolipin model membranes was studied to obtain insight into the stoichiometry of the lipid–protein complex. Cardiotoxin added to cardiolipin MLV caused an immediate precipitation of the lipid, which appeared to be accompanied by a high-affinity binding of cardiotoxin to the cardiolipin (Figure 1). From the results of the binding assay a cardiolipin to cardiotoxin molar ratio of 4.0 ± 0.1 can be calculated. Taking into account the double charge of the cardiolipin molecule, this value is in good agreement with earlier results (Dufoucq et al., 1978; Vincent et al., 1978) that showed ratios of one molecule of cardiotoxin vs. seven plus or minus one negative charges in phosphatidylinositol-containing, phosphatidylserine-containing, and phosphatidic acid containing systems. Additional experiments showed that the same stoichiometry of 4.0 ± 0.1 was found

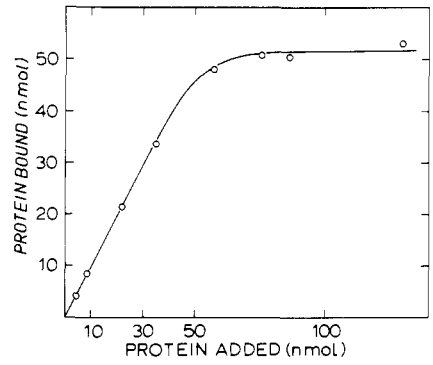

FIGURE 1: Binding of CTX II to MLV of beef heart cardiolipin. The amount of protein is given in nanomoles of protein per 200 nmol of cardiolipin. The estimated errors in the individual data points are 5–8%. Experimental conditions are as described under Materials and Methods.

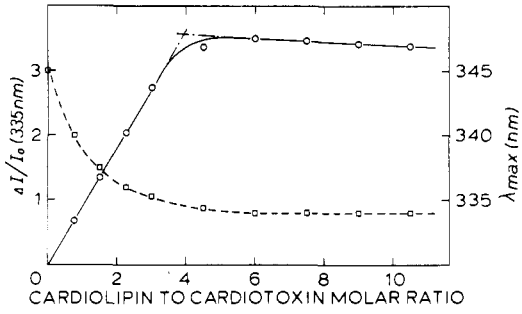

FIGURE 2: Effect of binding of CTX II to cardiolipin SUV on tryptophan fluorescence intensity (○) and wavelength of maximal fluorescence (□). Experimental detail is given under Materials and Methods. I_0 is the initial intensity, and ΔI is the increase of intensity after lipid addition.

if cardiotoxin was not added to the outside of cardiolipin MLV but instead was present in the buffer in which the lipid film was hydrated. Thus it appears, in contrast for instance to cytochrome *c* binding to cardiolipin MLV (Rietveld et al., 1983), that there are no pools of cardiolipin in the MLV inaccessible to cardiotoxin added at the outside.

Fluorescence Experiments. Tryptophan fluorescence reflects the environment in which the indole group is located and can therefore in principle be used to monitor the transfer of parts of proteins from an aqueous to an intramembranous location. Upon addition of cardiolipin SUV to cardiolipin, a blue shift and a marked increase of intensity of the fluorescence are observed (Figure 2), both indicating a more hydrophobic surrounding of tryptophan-11. Since binding to lipids did not appear to influence protein structure (Pézolet et al., 1982), this effect presumably is not caused by a burying of the indole group inside the protein but is rather a result of penetration of at least a part of the protein into the lipid matrix. The increase of intensity reaches a plateau at a cardiolipin to CTX II molar ratio of 3.8 ± 0.2 (mean of five independent measurements), which agrees well with the stoichiometry established by the binding studies. A K_D of (5 ± 1) × 10^{-8} M was calculated with an iterative nonlinear regression method as described previously (Hille et al., 1981) using the equation $K_D = [P][L_N][PL_N]^{-1}$, where [P] and [L] are the concentrations of the free protein and free lipid, respectively, and N is the amount of lipid monomers constituting one binding site for CTX II.

In order to further characterize the penetration of CTX II into cardiolipin vesicles, the ability of a membranous indole fluorescence quencher, anthracene, to quench the fluorescence of membrane-bound CTX II was examined. Anthracene in-

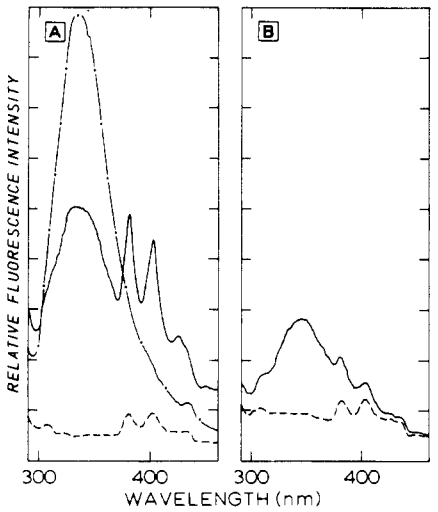

FIGURE 3: Emission spectra before (--) and after (—) addition of CTX II to anthracene incorporated in SUV of cardiolipin (A) or egg PC (B) and (-·-) after addition to cardiolipin SUV containing no anthracene. Concentrations: CTX, II 3.5 μM; anthracene, 1.75 μM; lipid, 140 μM (on basis of lipid phosphorus).

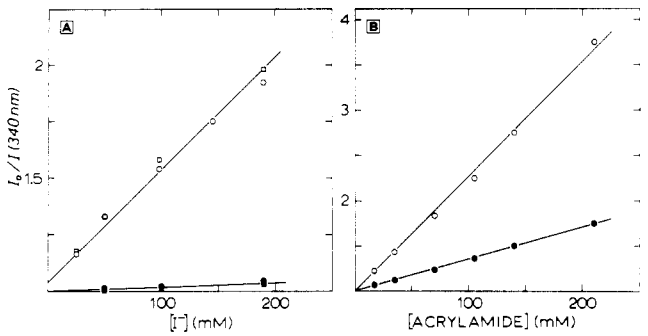

FIGURE 4: Stern–Volmer plots of the quenching of CTX II tryptophan fluorescence by jodide (A) or acrylamide (B) in the absence (○, □) or presence (●, ■) of cardiolipin. Initial concentrations: CTX II, 10 μM; cardiolipin, 500 μM.

corporated in cardiolipin SUV was able to quench tryptophan-11 fluorescence of added CTX II in a very efficient way (Figure 3A). Moreover, the intensity of the anthracene fluorescence peaks around 400 nm is much increased, due to resonance energy transfer from tryptophan to anthracene, which provides the basis of the quenching process. No such energy transfer is observed if CTX II is added to anthracene incorporated in egg PC vesicles (Figure 3B) to which cardiotoxin is not able to bind (Dufourcq et al., 1978; Vincent et al., 1978).

More direct information about the localization of the tryptophan residue can be obtained by studying the influence of collisional quenchers on fluorescence intensity. The quenching efficiency of the charged aqueous quencher I^- appeared to be decreased dramatically in the presence of lipid (Figure 4A), indicating a (nearly) complete shielding of the tryptophan from its original aqueous environment. Acrylamide's quenching efficiency is diminished by a factor of only 3 or 4 (Figure 4B), which is in agreement with the notion that this quencher can partition into the hydrophobic interior of the membrane (Cavatorta et al., 1982).

Structural Analysis. Phosphorus-31 NMR provides a very useful tool for the discrimination between phospholipid structures in natural and model membranes. ^{31}P NMR of pure cardiolipin MLV shows a spectrum with a dominating high-field peak and a low-field shoulder, characteristic of a random collection of bilayers in which the lipid phosphates undergo

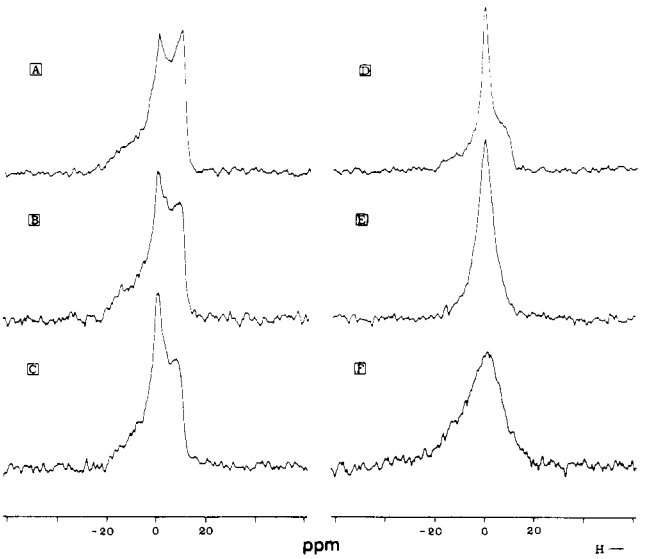

FIGURE 5: ^{31}P NMR spectra of MLV of cardiolipin before (A) and after (B–F) addition of increasing amounts of CTX II. CTX II to cardiolipin molar ratio: 1:40 (B); 1:30 (C); 1:20 (D); 1:10 (E); 1:3.5 (F). 0 ppm represents the chemical shift position of the signal of egg PC SUV.

rapid axial motion (Seelig, 1978). On this spectrum a small isotropic peak is superimposed, which most likely represents cardiolipin in small vesicles. This isotropic component is common to cardiolipin suspensions (de Kruijff et al., 1981; Rietveld et al., 1983). Upon addition of CTX II, no net changes in the spectrum are observed until a cardiolipin to CTX II ratio of about 50 is reached. Adding more CTX II results in a gradual increase of the contribution of the isotropic component to the spectrum (Figure 5B–E); at a molar ratio of 10, all phospholipid molecules show isotropic motion. If the amount of cardiotoxin is still further increased to a level at which all cardiolipin is saturated with peptide, the isotropic signal is very much broadened, indicating decreased headgroup mobility (Figure 5F).

At none of the ratios studied is any evidence for the existence of a hexagonal H_{II} phase, indicated by a low-field peak and high-field shoulder and a reduced line width (Seelig, 1978; de Kruijff et al., 1985) obtained from the spectra. It should be stressed again that no detectable cardiolipin degradation had taken place during these NMR experiments.

Unfortunately, ^{31}P NMR is not able to discern the different phospholipid structures in which the molecules can undergo rapid isotropic motion (SUV, micelles, inverted micelles, cubic phases). Though some of these structures can be ruled out (SUV, micelles) in view of the macroscopically large aggregates formed, additional techniques are still required to obtain a better understanding of the nature of the CTX II induced changes in phospholipid structure. In particular freeze–fracture electron microscopy and small-angle X-ray diffraction have proven to be useful in studies of lipid structure.

Small-angle X-ray diffraction of a CTX II–cardiolipin 1:20 complex (Figure 6A) shows rather diffuse reflections around 68 and 34 Å, interpretable as the first- and second-order reflections arising from stacked lamellar structures. The diffuse character of these peaks, which sharpen up in time at a time scale of hours, indicates that the stacking of the bilayers is not completely regular and that the distance between the lamellae is somewhat variable in contrast to the poly(L-lysine)–cardiolipin system (B. de Kruijff, unpublished observation). The fact that the starting material consisted of small single-walled SUV indicates a rigorous reorganization of the

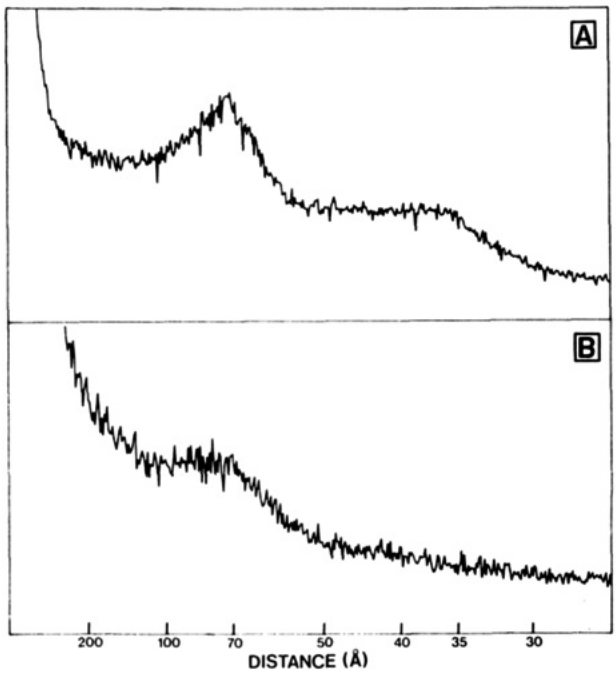

FIGURE 6: Small-angle X-ray diffraction patterns of CTX II–cardiolipin complexes. CTX II was added to cardiolipin SUV in a molar ratio of 1:20 (A) and 1:3.5 (B).

lipids, although a lamellar structure is conserved at least for the material showing some degree of order, in agreement with NMR data on mixtures of this ratio (Figure 5D). Cardiolipin saturated with CTX II shows no clear small-angle X-ray diffraction bands (Figure 6B) and thus no detectable order within the resolution limits of the technique.

In agreement with early observations (Gulik-Krywicki et al., 1981) on a phosphatidylserine- and phosphatidylethanolamine-containing natural mixture of phospholipids, addition of CTX II to cardiolipin SUV caused dramatic changes in freeze–fracture morphology. Besides the formation of extended stacked bilayers, well-defined particulate structures of about 10 nm in diameter and some tubular structures are visible on the bilayer fracture faces (Figure 7A,B). Most particles appear not to be randomly distributed in the bilayer planes but rather tend to stick together, sometimes forming hexagonally stacked arrays. The occurrence of pits complementary to the particles points to a lipidic nature of these particles (Verkleij et al., 1979). Another type of particles of less-defined diameter can also be observed that seem to represent cross sections through short channels connecting two aqueous compartments (Figure 7C). The amount of particles increases as the cardiolipin to CTX ratio decreases, and when the lipid is saturated with cardiotoxin, no smooth fracture faces can be seen anymore. Freeze–fracture under these conditions shows large areas of indistinctly ordered granular material, the size of the granules being variable and smaller than those of the well-defined particles mentioned above (Figure 7D).

It should be emphasized that all these observations were made on systems quenched in an ultrafast freezing device without the use of cryoprotectants. Possible artifacts that have been correlated to the presence of, for instance, glycerol (Boni et al., 1981) are thus avoided. If the cardiotoxin–cardiolipin complexes are frozen with the conventional methods after addition of 30% glycerol as cryoprotectant, partly different freeze–fracture images are obtained. When the lipid is saturated with protein, the cryoprotectant appears not to change the granular structure. However, if a subsaturating amount of CTX II is added to cardiolipin vesicles, freeze–fracture

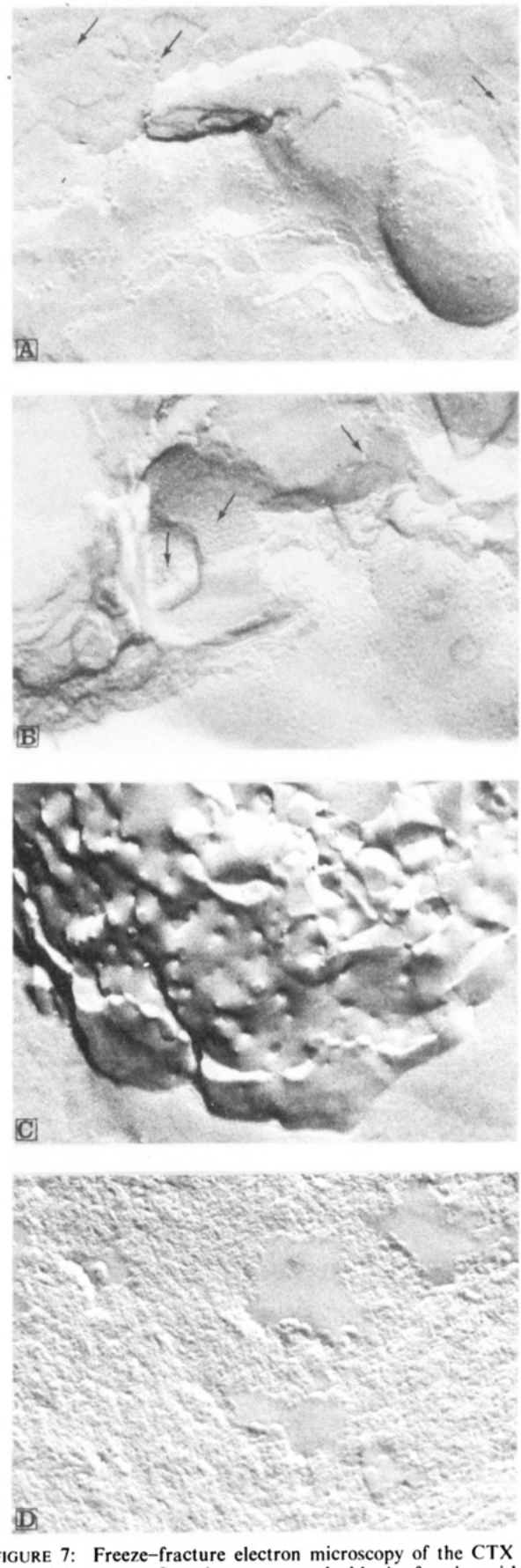

FIGURE 7: Freeze–fracture electron microscopy of the CTX II–cardiolipin system. Samples were quenched by jet-freezing without the use of cryoprotectants. CTX II to cardiolipin molar ratio 1:40 (A–C) and 1:3.5 (D); "pits" indicated by an arrow; magnification 81900×. Note the presence of tubular structures and well-defined particles (A), sometimes organized in close-packed arrays (B). Particles of less defined diameter are shown in (C).

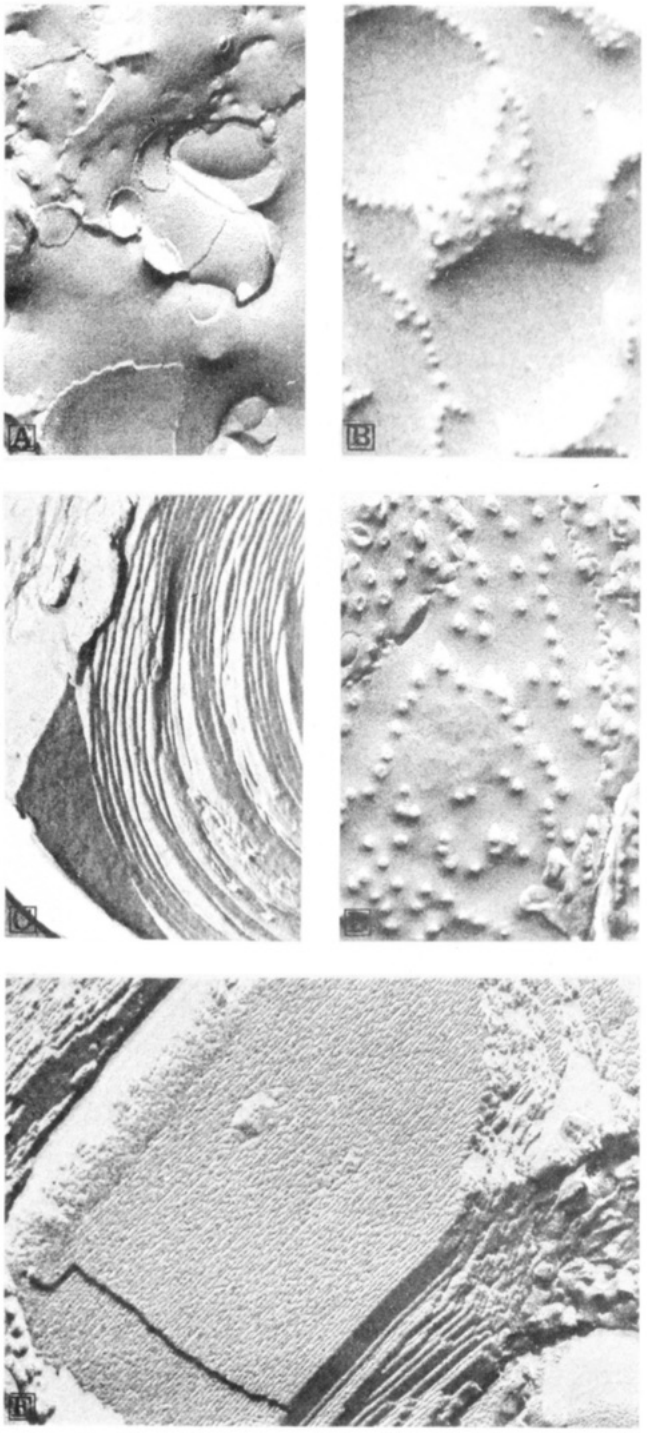

FIGURE 8: Freeze–fracture electron microscopy of the CTX II–cardiolipin system. Samples were frozen with 30% glycerol as cryoprotectant. Molar ratio 1:20; magnification 70000× [(E) 90000×]. Stacking of lamellae is shown in (A) and in cross section in (C). Note the presence of well-defined and less defined particles and pits (A, B, and D) and the occurrence of H_{II} phase (E).

(Figure 8) now shows not only the stacked bilayers and both kinds of particles mentioned earlier but also large stretches of well-ordered H_{II} phase (tube diameter 55 Å), which were absent after jet-freezing without glycerol. The structural data indicate an inverted nonbilayer structure of the formed CTX II–cardiolipin complex. To test this possibility, we studied the extractability into an organic phase of CTX II in the presence of cardiolipin using the method described under Materials and Methods. Cardiolipin (480 nmol of P_i) is able to transfer 93% (18.5 nmol) of the protein into the organic phase whereas no detectable CTX is extracted if no lipid is present or when

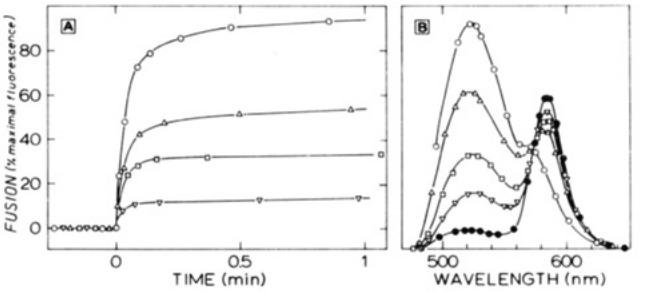

FIGURE 9: CTX II induced fusion of cardiolipin SUV as observed with the assay based on lipid mixing. CTX II was added as a 250 μM solution to 25 μM cardiolipin in a final volume of 2 mL. CTX II to cardiolipin molar ratio: 1:50 (▽); 1:20 (□); 1:10 (▲); 1:3.5 (○). In (B), the emission spectrum is shown 5 min after CTX II addition. The closed circles represent the spectrum before CTX II addition.

cardiolipin is replaced by egg PC. The observation that CTX II can be extracted in the presence of cardiolipin and not in its absence proves that CTX II and cardiolipin together can form chloroform-soluble complexes, compatible with an inverted micellar structure of the particles found on the fracture planes of cardiolipin bilayers in the presence of CTX II. It is noteworthy that phosphatidylglycerol, which has much less tendency to form inverted structures than cardiolipin (de Kruijff et al., 1985), extracts CTX II into an organic phase in a much less efficient way (31% or 6.1 nmol extracted by 440 nmol of lipid).

Fusion Studies. Both X-ray diffraction and freeze–fracture electron microscopy revealed that small unilamellar vesicles were transformed by the action of the cardiotoxin to large extended sheets of bilayer structure. This structural reorganization can only be accomplished by some kind of a fusion event. The kinetics of this fusion were studied by fluorescence techniques, monitoring either the mixing of the lipids (Struck et al., 1981) or the mixing of aqueous contents (Wilschut et al., 1980) of two different vesicle populations.

The mixing of the lipids is observed as a decrease of efficiency of resonance energy transfer between two probes incorporated into a minor part of the vesicles, due to dilution of the lipids upon fusion with a major nonfluorescent vesicle population. Such a decrease of energy-transfer efficiency is indeed seen after addition of CTX II to cardiolipin SUV (Figure 9). The initial rate of fusion appears to be extremely fast ($t_{1/2}$ in the order of seconds), but a complete mixing of the lipids is only achieved within the time course studied when a saturating amount of protein is added. It should be mentioned, however, that even CTX II added to a molar ratio of 1:50 was able to increase the 530-nm fluorescence up to 70% of the maximally possible value after prolonged incubation for 24 h, indicating that the fusion observed is biphasic rather than limited. Experiments with large unilamellar vesicles prepared with the reverse-phase evaporation technique gave similar results though with a 5–10 times slower initial rate of fusion (data not shown).

With the assay based on mixing of vesicle contents it is possible to see if the barrier properties of the vesicles are conserved throughout the fusion process; in other words, it is possible to discriminate between "leaky" and "nonleaky" fusion. During CTX II induced fusion of cardiolipin LUV with exactly the same lipid and CTX II concentrations as in the lipid-mixing assay, no formation of a fluorescent complex of Tb^{3+} and dipicolinic acid originally enclosed in different vesicle populations could be observed, not even temporarily as in the case of Ca^{2+}-induced fusion of cardiolipin–PC mixed vesicles (Wilschut et al., 1982) and of pure cardiolipin vesicles (unpublished observations). Fusion in the absence of EDTA in

the surrounding medium did however result in the formation of such a complex on a time scale comparable to that of lipid mixing, indicating that the barrier properties of the bilayers are affected in such a way that molecules as large as EDTA or the Tb^{3+}–dipicolinic acid complex can leak in or out.

Discussion

Our experiments show a strong interaction of CTX II with cardiolipin model membranes resulting in macroscopically large precipitates. The dissociation constant $K_D = 5 \times 10^{-8}$ M is in the same range as those of the cardiotoxin–phosphatidylinositol, –phosphatidylserine, and –phosphatidic acid complexes (Dufourcq & Faucon, 1978). Binding as well as fluorescence experiments showed a stoichiometry of one CTX II molecule bound to four doubly charged cardiolipin molecules. Since the protein has a net charge of 10+, this binding leads to compensation of most charges in the protein–lipid complex though no complete charge neutralization occurs in the protein-saturated complex as in the case of poly(L-lysine) binding to cardiolipin (de Kruijff & Cullis, 1980a).

The electrostatic interaction of the cardiotoxins with negatively charged lipids is accompanied by a certain degree of penetration into the lipid environment as suggested by tryptophan fluorescence (Vincent et al., 1978; Dufourcq & Faucon, 1978), monomolecular film technique (Bougis et al., 1981), differential scanning calorimetry, Raman spectroscopy, and fluorescence polarization (Faucon et al., 1983). The first part of this study describes a further characterization of this penetration in the CTX II–cardiolipin system. First, it was established that the tryptophan fluorescence behavior was affected by binding to cardiolipin model membranes in a way similar to the changes induced by binding to phosphatidylserine, phosphatidylinositol, and phosphatidic acid vesicles. The blue shift indicates a less polar environment of the tryptophan, and the intensity increase must be due to a decreased efficiency of the quenching by the water molecules. The increase of intensity is relatively large if compared to, for instance, apocytochrome *c* (A. Rietveld, unpublished data) and melittin (Dufourcq & Faucon, 1977) binding to phospholipids. A deep penetration of at least the tryptophan-containing part of the protein into the hydrophobic core of the lipids is pointed out by the efficient resonance energy transfer from tryptophan to the hydrophobic probe anthracene (Figure 3). A quantitative interpretation using Förster's equation (Förster, 1960) and an R_0, the distance of 50% energy transfer, of 19 Å as calculated for energy transfer from tryptophan to anthracene derivatives (Haigh et al., 1979) leads to an interprobe distance of 20 Å. Taking into account the surface density of the acceptor (0.012 mol/mol of P_i), the efficient (ca. 40%) energy transfer cannot be accomplished by anthracene molecules in one monolayer only, following the formalism of Fung & Stryer (1978) for two-dimensional Förster's theory of fluorescence energy transfer and the theoretical curves derived from it. Hence, a position of the tryptophan in the center of the hydrophobic core, allowing quenching by anthracene in both monolayers, is suggested. However, such calculations should be applied with much care, in view of, first, the relative insensitivity of the energy-transfer process to differences in vectorial distribution of the probes in case of a low surface density of donor and acceptor and, second, the uncertainty in the various parameters involved, especially the exact acceptor location and the dipole–dipole orientation factor, which was here assumed to be $^2/_3$. It is therefore more adequate to interpret the results by comparison with other protein–lipid systems. In this respect it is useful to mention that the efficiency of resonance energy transfer is of the same order of magnitude as in the case of the blocked dipeptide Boc-Trp-Phe-OEt completely partitioned into anthracene-labeled dipalmitoylphosphatidylcholine liposomes (Uemura et al., 1983).

Collisional quenchers of tryptophan fluorescence provide more straightforward information about the location of this residue, for only those quenchers that can come into physical contact with the indole group are able to decrease its fluorescence intensity. The traditional aqueous quencher I^- (Lehrer, 1971) appears to be able to quench the tryptophan fluorescence of cardiotoxin in the absence of lipid, indicative of an exposure of the indole group to the solvent. If the protein is bound to cardiolipin on the other hand, the Stern–Volmer plot (Figure 4A) shows clearly that the CTX II tryptophan is very efficiently shielded from the charged quencher. When this degree of shielding is compared with that in dimyristoylphosphatidylcholine of mellitin's tryptophan, which is probably situated in the glycerol area of the lipids (Vogel, 1981), it again indicates a deeper burying of the fluorophore. In agreement with this finding is the decreased ability of acrylamide to quench CTX II's tryptophan fluorescence.

All these quenching data confirm the concept of an insertion of the protein molecule deep into the hydrophobic environment of the lipid acyl chains. This correlates well with earlier Raman and fluorescence anisotropy results (Faucon et al., 1983), which showed strong influence on lipid acyl chain order.

The structural data presented in this study indicate a strong influence of CTX II on the macroscopic organization of the lipids to which it is bound. The effects of CTX II at lower, subsaturating, protein to lipid ratios will be considered first. ^{31}P NMR showed here the appearance of an isotropic signal, consistent with a fast reorientation of the lipid molecules with respect to the magnetic field, which points to small and highly curved structures if we assume the local structure of the phosphate region to be conserved. This signal cannot be attributed to micelles or small vesicles because a short centrifugation gives a complete recovery of the lipid in the pellet. Freeze–fracture of a system of comparable, low protein to lipid ratio shows, besides a stacking of bilayers, confirmed by X-ray data, the formation of large particles (≈100 Å) on the fractured bilayers, accompanied by complementary pits. The size of the particles makes it unlikely that these particles are formed by one protein molecule, but the possibility of protein aggregates sandwiched between the two monolayers cannot be completely ruled out. The uniform size of the particles, however, makes an at least partial lipidic character of these structures more easily conceivable. Evidence in favor of an inverted micellar structure is derived from two experiments. First, it was shown that cardiolipin is able to extract the protein into an organic phase, proving that a chloroform-soluble complex can be formed, most easily imaginable as an inverted lipidic structure encapsulating the polar part of the protein. Second, it was found that addition of glycerol to a 1:20 CTX II–cardiolipin complex resulted in the formation of the inverted hexagonal H_{II} phase. This H_{II} phase formation is not observed after addition of glycerol to pure cardiolipin and must therefore be related to the tendency of the cardiotoxin–cardiolipin complex itself to form inverted structures, which is intensified when the surrounding water is replaced by glycerol. This idea is in agreement with the common observation of lipidic particles (or isotropic peaks in NMR) in situations intermediate between bilayer and H_{II} phase. At higher protein to lipid ratios, the contribution of the broad isotropic component in the NMR spectrum becomes larger, and at a cardiolipin to cardiotoxin molar ratio of 10, thus clearly before saturation of the lipid, no bilayer spectrum is observed anymore. Further

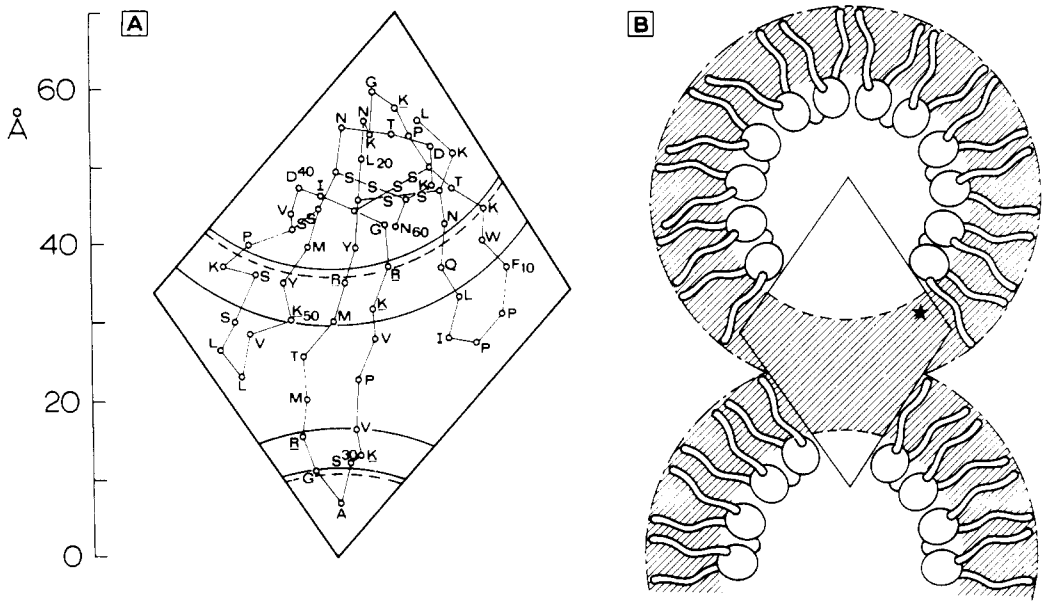

FIGURE 10: α-Carbon diagram of CTX II, based on the X-ray structure of the neurotoxin erabutoxin b from *Laticauda semifasciata* (Tsernoglou & Petsko, 1976) (A) and a schematic drawing of the structure proposed for the CTX II–cardiolipin complex (B). In (A), two zones rich in α-carbon atoms of positively charged residues (underlined) are indicated. The dotted lines mark the boundaries of the hydrophobic region, assuming a complete stretching of the side chains of lysine-50 and arginine-27 in opposite directions. The shaded area in (B) represents the hydrophobic region of lipids and protein; the position of the tryptophanyl residue is indicated by a star. IUPAC one-letter code: A = Ala; C = Cys; D = Asp; E = Glu; F = Phe; G = Gly; H = His; I = Ile; K = Lys; L = Leu; M = Met; N = Asn; P = Pro; Q = Gln; R = Arg; S = Ser; T = Thr; Y = Tyr; V = Val; W = Trp.

addition of CTX II to a saturating level causes a further broadening of the isotropic peak, pointing to a decreased mobility, a restricted possibility of reorientation of the lipid molecules. In this situation electron microscopy merely shows stretches of granular material, which no longer can be converted into an H_{II} organization by addition of 30% glycerol. The grains are of an irregular size and packing, and this lack of order is further underlined by small-angle X-ray diffraction.

The small-angle X-ray diffraction and electron microscopy results indicate a CTX II induced fusion of the cardiolipin vesicles. This fusion process, when monitored with a lipid mixing based fusion assay, is initially extremely fast and efficient, taking into account the micromolar range of fusogen concns. used, but slows down abruptly after some 5 s. This may be related to the high lipid affinity ($K_D \sim 10^{-7}$ M) of CTX II, which, added as a concentrated solution, is not able, in spite of the thorough stirring, to reach all vesicles, leading to heterogeneity among the lipid structures as reflected earlier in the freeze–fracture morphology of cardiolipin treated with subsaturating amounts of CTX II. Study of mixing of aqueous vesicle contents pointed to a "leaky" kind of fusion. It is of interest to correlate the fusion phenomenon with the features observed by electron microscopy. In this respect it is worth noticing the vulcano-like particles especially clear in the samples frozen with glycerol, but also present after jet-freezing, protrusions of a large and very variable size with a flat or somewhat invaginated top. These structures have been proposed to represent the aqueous channels connecting the vesicles in the last stage of a fusion process, the so-called "fission" step (Verkleij, 1984). The well-defined particles mentioned earlier, most likely representing inverted micelles, could also play a role as intermediate structures during fusion at a point of connection of two "joining" bilayers (Cullis et al., 1983; Verkleij et al., 1980), though it should be admitted that the involvement of inverted micelles in membrane fusion processes is not generally accepted (Hui et al., 1981; Bearer et al., 1982).

Another point of interest is the location of the protein molecules in the structures formed. Two models for cardiotoxin–acidic lipid interaction have been proposed. In one of them (Dufourcq et al., 1982) only one of the β-pleated loops of the peptide interacts with the hydrophobic interior of the membrane. In an alternative model (Lauterwein & Wüthrich, 1978) all three hydrophobic loops are proposed to be inserted into the membrane, the central loop crossing the bilayer, thereby exposing the charged residues on its tip for interaction with lipid phosphates at the opposite side of the bilayer. If the bilayer is assumed to be curved, this situation would allow eight positively charged amino groups bordering the hydrophobic β-sheet to be salt-bridged in the polar region of the lipid head groups (Lauterwein & Wüthrich, 1978). This model, more than the previously mentioned alternative, accounts for the high affinity and the stoichiometry of the binding and the specificity when compared, for instance, with the neurotoxins, which have a similar tertiary structure but a different amino acid composition and which do not show interaction with phospholipids (Faucon et al., 1979). A serious disadvantage of this model is the mismatch between the length of the hydrophobic region of the protein and the thickness of the hydrophobic core of a lipid bilayer, even when the lysine and arginine side chains on either side of the hydrophobic part are assumed to point to opposite directions, thereby enlarging the hydrophobic part from 14 to 26 Å. Neither of the two models takes into account the morphological changes described in this study. We therefore propose for the CTX II–cardiolipin complex a third alternative, in fact based on the former ones, which is schematically represented in Figure 10. The protein resides with its polar part, containing the disulfide bridges in the interior of an inverted micelle, the zone of positively charged residues at the interface, and its hydrophobic β-pleated sheet in the acyl chain region. In the outlined situation, the lipids better accommodate the length of the protein's hydrophobic region due to a decreased dynamic length of the acyl chains or a certain degree of interdigitation of these chains. This model can furthermore account for the observed well-defined lipidic particles and the solubility in chloroform of the CTX II–cardiolipin complex. The tryptophan residue would

be situated in the acyl chain region of the lipids in accordance with the fluorescence data.

Summarizing, the driving force for the formation of the outlined structures would be supplied by the spacial distribution of polar, charged, and hydrophobic residues, including the inability to span the hydrophobic core of a bilayer and the clearly rhombic shape of the peptide molecule. Considerations of shape and mismatch of hydrophobic length have been used earlier to explain the induction of an inverted phase in neutral lipid systems by gramicidin (Van Echteld et al., 1982). Evidently, however, in the case of the cardiotoxins the electrostatic interaction of the stategically situated lysines and arginines with the acidic lipid's phosphates, leading to reduced inter head group repulsion and hence (de Kruijff et al., 1984) increased H_{II} phase tendency, has an essential contribution to the binding and morphological changes and explains the exclusive interaction with negatively charged phospholipids. In this respect a comparison with positively charged apocytochrome *c*, the precursor of mitochondrial cytochrome *c*, which causes similar morphological changes in cardiolipin- and phosphatidylserine-containing lipid systems (Rietveld et al., 1983), is more obvious. It would be of great biological relevance to see if these morphological changes can be related to the insertion and translocation of precursors of membrane and secretory proteins in general and what role the leader peptide with its clusters of positively charged and hydrophobic residues may play. Experiments with other model peptides of clearly defined tertiary structure and synthetically prepared leader sequences will be necessary to answer this question.

ACKNOWLEDGMENTS

We thank J. Leunissen-Bijvelt for carrying out the freeze–fracture experiments and J. C. L. Hibbeln for his part of the fusion assays.

REFERENCES

Bearer, E. L., Düzgünez, N., Friend, D. S., & Papahadjopoulos, D. (1982) *Biochim. Biophys. Acta 693*, 93–102.

Boni, L. T., Steward, T. P., Aldorfer, J. L., & Hui, S. W. (1981) *J. Membr. Biol. 62*, 65–70.

Bougis, P., Rochat, H., Pieroni, G., & Verger, R. (1981) *Biochemistry 20*, 4915–4920.

Bougis, P., Tessier, M., van Rietschoten, J., Rochat, H., Faucon, J. F., & Dufourcq, J. (1983) *Mol. Cell. Biochem. 55*, 49–64.

Cavatorta, P., Spisni, A., Casali, E., Lindner, L., Masotti, L., & Urri, D. W. (1982) *Biochim. Biophys. Acta 689*, 113–120.

Comfurius, P., & Zwaal, R. F. A. (1977) *Biochim. Biophys. Acta 488*, 36–42.

Cullis, P. R., & de Kruijff, B. (1976) *Biochim. Biophys. Acta 506*, 173–182.

Cullis, P. R., & Hope, M. J. (1978) *Nature (London) 271*, 672–674.

Cullis, P. R., de Kruijff, B., Hope, M. J., Verkleij, A. J., Nayar, R., Farren, S. B., Tilcock, C., Madden, T. D., & Bally, M. B. (1983) in *Membrane Fluidity* (Alioa, R. C., Ed.) Vol. 2, pp 40–79, Academic Press, New York.

Dassaux, J. L., Faucon, J. F., Lafleur, M., Pézolet, M., & Dufourcq, J. (1984) *Biochim. Biophys. Acta 775*, 37–50.

de Kruijff, B., & Cullis, P. R. (1980a) *Biochim. Biophys. Acta 601*, 235–240.

de Kruijff, B., & Cullis, P. R. (1980b) *Biochim. Biophys. Acta 602*, 477–490.

de Kruijff, B., Verkleij, A. J., van Echteld, C. J. A., Gerritsen, W. J., Noordam, P. C., Mombers, C., Rietveld, A., de Gier, J., Cullis, P. R., Hope, M. J., & Nayar, R. (1981) in *International Cell Biology 1980–1981* (Schweiger, H. G., Ed.) pp 559–571, Springer Verlag, Berlin.

de Kruijff, B., Cullis, P. R., Verkleij, A. J., Hope, M. J., van Echteld, C. J. A., & Taraschi, T. F. (1985) in *The Enzymes of Biological Membranes* (Martinosi, A., Ed.) pp 131–204, Plenum, New York.

Delori, P., & Tessier, M. (1980) *Biochimie 62*, 287.

Dufourcq, J., & Faucon, J. F. (1977) *Biochim. Biophys. Acta 467*, 1–11.

Dufourcq, J., & Faucon, J. F. (1978) *Biochemistry 17*, 1170–1176.

Dufourcq, J., Faucon, J. F., Bernard, E., Pézolet, M., Tessier, M., Bougis, P., van Rietschoten, J., Delori, P., & Rochat, H. (1982) *Toxicon 20*, 165–174.

Dufton, M. J., & Hider, R. C. (1983) *Crit. Rev. Biochem. 14*, 115–171.

Faucon, J. F., Dufourcq, J., Couraud, F., & Rochat, H. (1979) *Biochim. Biophys. Acta 554*, 332–339.

Faucon, J. F., Bernard, E., Dufourcq, J., Pézolet, M., & Bougis, P. (1981) *Biochimie 63*, 857–861.

Faucon, J. F., Dufourcq, J., Bernard, E., Duchesneau, L., & Pézolet, M. (1983) *Biochemistry 22*, 2179–2185.

Fiske, C. H., & Subbarow, Y. (1925) *J. Biol. Chem. 66*, 375–389.

Förster, T. (1960) *Radiat. Res., Suppl. 2*, 326–339.

Fung, B., & Stryer, L. (1978) *Biochemistry 17*, 5241–5248.

Gulik-Krzywicki, T., Balerna, M., Vincent, J. P., & Lazdunski, M. (1981) *Biochim. Biophys. Acta 643*, 101–114.

Haigh, E. A., Thulborn, K. R., & Sawyer, W. H. (1979) *Biochemistry 18*, 3525–3532.

Hille, J. D. R., Donné-Op den Kelder, G. M., Sauve, P., de Haas, G. H., & Egmond, M. R. (1981) *Biochemistry 20*, 4068–4073.

Hui, S. W., Steward, T. P., Boni, L. T., & Yeagle, P. L. (1981) *Science (Washington, D.C.) 212*, 921–922.

Killian, J. A., Leunissen-Bijvelt, J., Verkleij, A. J., & de Kruijff, B. (1985) *Biochim. Biophys. Acta 812*, 21–26.

Lauterwein, J., & Wüthrich, K. (1978) *FEBS Lett. 93*, 181–184.

Lehrer, S. S. (1971) *Biochemistry 10*, 3254–3263.

Louw, A. I. (1974) *Biochim. Biophys. Acta 336*, 481–495.

Nesmeyanova, M. A. (1982) *FEBS Lett. 142*, 189–193.

Peterson, G. L. (1977) *Anal. Biochem. 83*, 345–356.

Pézolet, M., Duchesneau, L., Bougis, P., Faucon, J. F., & Dufourcq, J. (1982) *Biochim. Biophys. Acta 704*, 515–523.

Pscheid, P., Schudt, C. S., & Plattner, H. (1981) *J. Microsc. (Oxford) 121*, 149–154.

Rietveld, A., Syens, P., Verkleij, A. J., & de Kruijff, B. (1983) *EMBO J. 2*, 907–913.

Rouser, G., Fleischer, S., & Yamamoto, A. (1975) *Lipids 5*, 494–496.

Seelig, J. (1978) *Biochim. Biophys. Acta 515*, 105–140.

Struck, D. K., Hoekstra, D., & Pagano, R. E. (1981) *Biochemistry 20*, 4093–4099.

Szoka, F. C., & Papahadjopoulos, D. (1978) *Proc. Natl. Acad. Sci. U.S.A. 75*, 4194–4198.

Taraschi, T. F., de Kruijff, B., Verkleij, A. J., & van Echteld, C. J. A. (1982) *Biochim. Biophys. Acta 601*, 235–240.

Taraschi, T. F., de Kruijff, B., & Verkleij, A. J. (1983) *Eur. J. Biochem. 129*, 621–625.

Tsernoglou, D., & Petsko, G. A. (1976) *FEBS Lett. 68*, 1–4.

Uemura, A., Kimura, S., & Imanishi, Y. (1983) *Biochim. Biophys. Acta 729*, 28–34.

Verkleij, A. J. (1984) *Biochim. Biophys. Acta 779*, 43-63.
Verkleij, A. J., Mombers, C., Leunissen-Bijvelt, J., & Ververgaert, P. H. J. Th. (1979) *Nature (London) 279*, 162-163.
Vincent, J. P., Schweitz, H., Clicheportiche, R., Fosset, M., Balerna, M., Leloir, M. C., & Lazdunski, M. (1976) *Biochemistry 15*, 3171-3175.
Vincent, J. P., Balerna, M., & Lazdunski, M. (1978) *FEBS Lett. 85*, 103-108.
Vogel, H. (1981) *FEBS Lett. 134*, 37-42.
Wilschut, J., Düzgünez, N., Fraley, R., & Papahadjopoulos, D. (1980) *Biochemistry 19*, 6011-6021.
Wilschut, J., Holsappel, M., & Jansen, R. (1982) *Biochim. Biophys. Acta 690*, 297-301.

Lateral Distribution of Phospholipid and Cholesterol in Apolipoprotein A-I Recombinants†

John B. Massey,* Hoyan S. She, Antonio M. Gotto, Jr., and Henry J. Pownall
Department of Internal Medicine, Baylor College of Medicine, and The Methodist Hospital, Houston, Texas 77030
Received June 19, 1985

ABSTRACT: The influence of cholesterol on the assembly and structure of model high-density lipoproteins (HDL) has been investigated. Model HDL composed of apolipoprotein A-I (apoA-I) and 1,2-dimyristoylphosphatidylcholine (DMPC) formed spontaneously at the transition temperature (T_c) of the lipid. Those composed of apoA-I and 1-palmitoyl-2-oleoylphosphatidylcholine were formed by a cholate dialysis method. At low cholesterol/phospholipid ratios both lipids and assembly methods yielded a model HDL whose composition was identical with that of the initial mixture; as the cholesterol/phospholipid ratio of the initial mixture was increased, the fraction of cholesterol appearing in the model HDL decreased, and a negative correlation between the cholesterol and protein contents of the model HDL was observed. At high cholesterol/phospholipid ratios the association of apoA-I and phospholipids appeared to be thermodynamically unfavorable. The effects of cholesterol content on the thermal properties of a model HDL composed of DMPC and apoA-I were further investigated by differential scanning calorimetry, fluorescence polarization of 1,6-diphenyl-1,3,5-hexatriene, fluorescence energy transfer, and excimer fluorescence of pyrenyl derivatives of phosphatidylcholine (PC) and cholesterol. The addition of cholesterol decreased the transition enthalpy of DMPC, raised the midpoint of the transition, and modulated motional freedom in the phospholipid matrix. The amount of cholesterol required to produce these effects was lower in the model HDL than in multilamellar liposomes. In a model HDL composed of DMPC and apoA-I, the lateral diffusion of a pyrene-labeled cholesterol was dramatically changed at the T_c whereas little change was observed in that of a pyrene-labeled PC. The relative locations of a fluorescent PC and cholesterol derivative in a model HDL were measured by fluorescence energy transfer from the tryptophan residues of the protein to the probe molecules. On the average, the fraction of cholesterol adjacent to the protein, though measurable, was less than that of the PC; therefore, the cholesterol is partially excluded from the phospholipid surrounding the protein but has the same modulating effect on the remainder of the phospholipid in the recombinant as that seen in multilayer liposomes. The effect of cholesterol on the reassembly of model lipoproteins appears to be due to the competition between cholesterol and apoA-I for "hydrophobic solvation" by the phospholipid. The results suggest that PC is preferentially included and cholesterol is partially excluded from the region adjacent to apoA-I.

Model high-density lipoprotein(s) (HDL)[1] formed by assembling apoA-I, PC, and cholesterol contains the minimal number of components required for an LCAT substrate (Fielding et al., 1972; Smith et al., 1978; Matz & Jonas, 1982a,b; Pownall et al., 1982b). Numerous studies using a variety of physicochemical techniques have focused upon the structure and properties of model HDL containing apoA-I and DMPC (Wlodawer et al., 1979; Jonas & Mason, 1981; Reijngould et al., 1982; Atkinson et al., 1980; Morrisett et al., 1977; Tall et al., 1977; Pownall, 1978, 1981). The model HDL have the morphology of a bilayer disk that is similar to those observed in the plasma of LCAT-deficient subjects (Forte et al., 1971) and from the perfused rat liver (Hamilton et al., 1976).

The effects of cholesterol on the assembly of model HDL have been studied in several laboratories. Addition of up to

† This investigation was supported by grants from the National Institutes of Health (HL27341, HL30913, and HL30914).
* Address correspondence to this author at the Department of Internal Medicine, Baylor College of Medicine.

[1] Abbreviations: HDL, high-density lipoprotein(s); PC, phosphatidylcholine; DMPC, 1,2-dimyristoylphosphatidylcholine; POPC, 1-palmitoyl-2-oleoylphosphatidylcholine; MPNPC, 1-myristoyl-2-[9-(1-pyrenyl)nonanoyl]phosphatidylcholine; MAUPC, 1-myristoyl-2-[11-(9-anthroyloxy)undecanoyl]phosphatidylcholine; LMPC, 1-myristoylphosphatidylcholine; AMC, 9-anthracenylmethyl 3β-hydroxy-22,23-bis(nor-5-cholenate); PMC, 1-pyrenylmethyl 3β-hydroxy-22,23-bis(nor-5-cholenate); AU, 11-(9-anthroyloxy)undecanoic acid; LCAT, lecithin:cholesterol acyltransferase; apoA-I, apolipoprotein A-I (the most abundant protein of human plasma high-density lipoproteins); DSC, differential scanning calorimetry; T_c, midpoint of gel to liquid-crystalline phase transition; ΔH, enthalpy of gel to liquid phase transition; M/M, molar ratio of lipid to protein; DPH, 1,6-diphenyl-1,3,5-hexatriene; EDTA, ethylenediaminetetraacetic acid; Tris, tris(hydroxymethyl)aminomethane.

0006-2960/85/0424-7110$01.50/0